This article has been accepted for publication in a future issue of this journal, but has not been fully edited. Content may change prior to final publication. Citation information: DOI 10.1109/TIA.2018.2867324, IEEE Transactions on Industry Applications

A Second-Order Volterra Filter Based Control of Solar PV-DSTATCOM System to Achieve Lyapunov's Stability

Neha Beniwal, *Student Member, IEEE,* Ikhlaq Hussain, *Member, IEEE* and Bhim Singh, *Fellow IEEE.*
Dept. of Electrical Engineering, Indian Institute of Technology Delhi, New Delhi, India
nsingh341@gmail.com, ikhlaqiitd@gmail.com and bsingh@ee.iitd.ac.in

***Abstract*— In this work, a Volterra filter based control algorithm is developed to generate reference currents for a solar PV-DSTATCOM (Photovoltaic-Distribution Static Compensator) system in the distribution network. The developed control is analyzed for being stable under Lyapunov stability criterion, consequently, the error function of the system converges to zero asymptotically. The PV-DSTATCOM system is integrated to the grid to compensate the nonlinear load while supplying solar PV array active power to the grid. The system is modeled in MATLAB and is executed on a developed prototype in the laboratory, under balanced, unbalanced loading conditions and variable insolation conditions. Moreover, the harmonic distortion of the grid currents, is observed under the IEEE-519 standard.**

Keywords*— *Volterra, Lyapunov's stability, Power Quality, PV, and DSTATCOM.

I. INTRODUCTION

With the growing demand of electricity, the world has seen a drastic shift towards distributed generation using renewable sources of energy [1-2]. The distributed generation not only reduces the burden on electrical grid, but also helps the consumers to participate in the energy market by selling the excess generated power. Solar energy, being one of the most abundant resources, has been a major research focus in the past two decades [3]. With the continuous decreasing costs and subsequent increasing incentives, solar PV (Photovoltaic) systems are installed worldwide in large numbers. However, the integration of solar PV systems to the conventional electrical grid, faces power quality challenges like [4-6],

- Harmonics- current and voltage harmonics are major concern as the solar PV converter acts as a harmonics injecting source in the grid.
- Fluctuations in voltage – an intermittent nature of solar PV generation (as solar power generation is determined by the operating temperature and irradiance levels), leads in voltage fluctuations.

An IEEE-519 standard has recommended the total harmonic distortion in grid currents to be lower than 5% [7]. Moreover, an IEEE-1547 standard recommends the voltage fluctuations at the point of common coupling (PCC) to be within ±5% [8]. Therefore, for the mitigation of the problems associated with the power quality and also to maintain the IEEE standards, it is important to develop the control of solar PV systems with improved performance.

The solar PV array is integrated to the grid using a DSTATCOM (Distribution Static Compensator), which is basically realized using a VSC (Voltage Source Converter). The solar PV array is operated to attain maximum power using various tracking techniques [9-10]. The most commonly used MPPT (Maximum Power Point Tracking) technique is an incremental conductance (IC) technique [11], wherein the current and voltage of the solar PV array, help in acquiring the operating point. An IC technique helps in obtaining true MPPT without periodic tuning, thus provides an easier method to obtain the maximum power point.

Other advantage of a solar PV- DSTATCOM (Photovoltaic-Distribution Static Compensator) system, is that in the absence of solar PV generation, the system has the capability to operate as a DSTATCOM unlike the traditional solar PV systems wherein zero solar PV generation implies idle system. The main features of a DSTATCOM are as follows [12-13].

- It help in correcting power factor at the grid side even with the load operating at poor power factor.
- It maintains sinusoidal grid currents even with non-sinusoidal load currents.
- It helps to draw balanced grid currents while feeding unbalanced loads.

These features of DSTATCOM remain intact while operating as a solar PV- DSTATCOM system, thus, it helps in mitigating the power quality issues.

Singh et al. [14] have reported numerous topologies for DSTATCOM. The major criteria for deciding the correct topology, are to have a compact, less bulky system and at the same time to minimize the switching losses. The most widely accepted topology is a nonisolated three-phase three-wire topology, as it doesn't contain bulky transformers and inductors. Moreover, the number of switches, is optimum to provide full control of grid currents and the voltage at the PCC.

The operation of a solar PV-DSTATCOM system is basically dependent on the switching pulses given to the VSC. The reference currents are used to generate pulses, which helps in compensating the reactive power, eliminating the harmonics and balancing the power at point of common coupling. The basic objective is to control these switching pulses to minimize the distortion in grid currents. Various control algorithms like Adaline based control, instantaneous reactive power theory (IRPT), synchronous reference frame theory (SRF), instantaneous p-q-r theory, composite observer based, etc. have been proposed in the literature [13,15-16]. SRF based control uses a PLL in transforming three phase quantities to two phases, and therefore, the system's PLL has to be tuned prior to its operation. Similar observation can be easily made for the SOGI-PLL proposed in [17], wherein distortions and noise easily affect the PLL performance. IRPT is implemented using the power of the system, which in turn is calculated from the voltages and the currents of the system. Consequently, fluctuations in the voltages, are reflected on the reference currents calculation. Instantaneous symmetrical component theory based control algorithm also makes use of power

This article has been accepted for publication in a future issue of this journal, but has not been fully edited. Content may change prior to final publication. Citation information: DOI 10.1109/TIA.2018.2867324, IEEE Transactions on Industry Applications

calculations and is subsequently affected by voltage fluctuations. A naive- back propagation based Icosϕ algorithm has been implemented for the DSTATCOM control in [18], however, rigorous calculations involved, make the algorithm complex and difficult to implement. Loubassou et al. [19] have developed kernel incremental metal learning algorithm to generate the reference grid currents. The control has less sensitivity to internal parameters variation. However, the performance of the control has not been analyzed on a hardware prototype. A nonlinear Volterra filter [20], being adaptive in nature can easily help in achieving the aim for the operation of a solar PV-DSTATCOM system. It is vital that the Volterra filter based control developed for the solar PV-DSTATCOM, should not result in an unstable system [21].

In this paper, a solar PV array is integrated to the grid, via a DSTATCOM. The operating point at maximum power of solar PV array is tracked using an IC algorithm. A second-order Volterra filter is used to estimate the reference currents from nonlinear load currents. A Lyapunov function based upon the error of the system is considered and the stability analysis is undertaken to ensure the system's performance under transient conditions as well [22-25]. The proposed control design is first modeled in MATLAB/Simulink environment and is then implemented in the laboratory. The proposed solar PV-DSTATCOM system is analyzed under load variation, load unbalancing and varying insolation and the obtained results are evaluated as per the IEEE-519 and the IEEE-1547 standards.

II. Proposed Topology

To operate the given system, the solar PV array is tied to the grid as depicted in Fig. 1. The solar PV system is modeled by using the procedure followed in [26] and uses IC-MPPT for extraction of maximum power. The VSC (Voltage Source Converter) is connected at the PCC via interfacing inductors (L_f) to control current ripples. On the other hand, to minimize voltage ripples, a ripple filter (R_f & C_f) is connected at PCC. The IGBTs (Insulated Gate Bipolar Transistors) of VSC, are controlled by an algorithm based upon second-order Volterra filter and improved with the Lyapunov's stability.

III. Control Approach

The control of PV-DSTATCOM system is shown in Figs. 2 and 3. The solar PV system operates at maximum power using an IC algorithm, which basically uses the power-voltage curve of PV array to determine the operating point [11].

The control of VSC is developed using a Volterra filter based control algorithm with the Lyapunov's stability. The Volterra filter helps to include the previous values of the system, thus adding the memory element to the system. The Volterra filter variables are adaptively changed based upon the Lyapunov's stability theory in order to converge the error to zero asymptotically.

First of all, the amplitude of terminal voltage (V_t) is calculated as [13],

$$V_t = \sqrt{\frac{2}{3}(v_{ga}^2 + v_{gb}^2 + v_{gc}^2)} \tag{1}$$

where v_{ga}, v_{gb} and v_{gc} are the grid phase voltages of the three phases, which are evaluated from the line grid voltages v_{gab} and v_{gbc} as,

$$v_{ga} = \frac{2v_{gab} + v_{gbc}}{3}; v_{gb} = \frac{-v_{gab} + v_{gbc}}{3}; v_{gc} = \frac{-v_{gab} - 2v_{gbc}}{3} \tag{2}$$

The V_t is then used to find the in-phase unit templates as,

$$u_{Aa} = \frac{v_{ga}}{V_t}; u_{Ab} = \frac{v_{gb}}{V_t}; u_{Ac} = \frac{v_{gc}}{V_t} \tag{3}$$

Moreover, using these in-phase templates, the quadrature-phase unit templates are evaluated as,

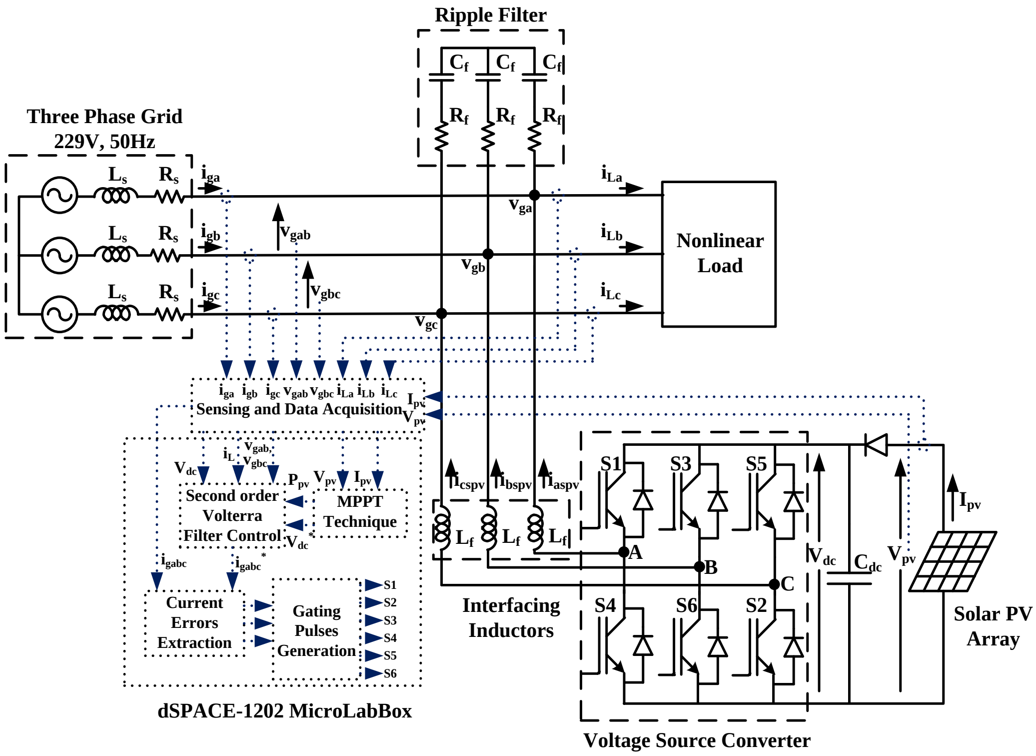

Fig. 1 Proposed system.

This article has been accepted for publication in a future issue of this journal, but has not been fully edited. Content may change prior to final publication. Citation information: DOI 10.1109/TIA.2018.2867324, IEEE Transactions on Industry Applications

$$u_{Ra}=\frac{-u_{Ab}+u_{Ac}}{\sqrt{3}};u_{Rb}=\frac{\sqrt{3}}{2}(u_{Aa}+\frac{u_{Ab}-u_{Ac}}{3});\quad u_{Rc}=\frac{\sqrt{3}}{2}(-u_{Aa}+\frac{u_{Ab}-u_{Ac}}{3}) \tag{4}$$

The current error of active component in each phase at nth instant is shown in Fig. 2 and is defined as,

$$e_{Am}(n)=i_{Lm}(n)-w_{Am}(n)*u_{Am}(n) \tag{5}$$

where m represents phases a, b and c individually.

The basic aim of the control is to minimize this mean square error. Here, $w_{Am}(n)$ varies in order to update the value of e_{Am} based like,

$$w_{Am}(n)=w_{Am}(n-1)-\varepsilon_{Am}(n)*\alpha_{Am}(n) \tag{6}$$

where $\alpha_{An}(n)$ represents the adaptation gain, $\varepsilon_{An}(n)$ is the priori estimation error and are given as,

$$\varepsilon_{Am}(n)=i_{Lm}(n)-w_{Am}(n-1)*u_{Am}(n) \tag{7}$$

$$\text{and } \alpha_{Am}(n)=-u_{Am}(n)\left[1-\delta\frac{|e_{Am}(n-1)|}{|\varepsilon_{Am}(n)|}\right] \tag{8}$$

where 0<δ<1.

Both $\alpha_{Am}(n)$ and $\varepsilon_{Am}(n)$ vary with time to minimize the error given in (5).

Thus, w_{Aa}, w_{Ab}, and w_{Ac}, are evaluated and are averaged to calculate the total-load weight component as,

$$w_{LAa}=\frac{w_{Aa}+w_{Ab}+w_{Ac}}{3} \tag{9}$$

The solar PV array power is used to find the PV weight component as,

$$w_{pv}(n)=\frac{2P_{pv}(n)}{3V_t} \tag{10}$$

The error defined by the difference of the reference DC link voltage and DC link voltage is fed to a PI (Proportional-Integral) controller to generate the DC link weight as,

$$w_{Ad}(n+1)=w_{Ad}(n)+K_{p1}\{e_d(n+1)-e_d(n)\}+K_{i1}e_d(n+1) \tag{11}$$

$$\text{where } e_d(n)=V_{dc}^*(n)-V_{dc}(n) \tag{12}$$

The total active in-phase weight is evaluated as,

$$w_{As}=w_{LAa}+w_{Ad}-w_{pv} \tag{13}$$

The w_{As} is then used to generate the active components of reference currents as,

$$i_{Aa}^*=u_{Aa}*w_{As};i_{Ab}^*=u_{Ab}*w_{As};i_{Ac}^*=u_{Ac}*w_{As} \tag{14}$$

At nth instant, the quadrature-phase error of the phases is given as,

$$e_{Rm}(n)=i_{Lm}(n)-w_{Rm}(n)*u_{Rm}(n) \tag{15}$$

where w_{Rm} is expressed as,

$$w_{Rm}(n)=w_{Rm}(n-1)-\varepsilon_{Rm}(n)*\alpha_{Rm}(n) \tag{16}$$

$$\text{such that } \varepsilon_{Rm}(n)=i_{Lm}(n)-w_{Rm}(n-1)*u_{Rm}(n) \tag{17}$$

$$\text{and } \alpha_{Rm}(n)=-u_{Rm}(n)\left[1-\delta\frac{|e_{Rm}(n-1)|}{|\varepsilon_{Rm}(n)|}\right] \tag{18}$$

where 0<δ<1.

The total reactive weight of load is calculated by taking a mean of three reactive load weights i.e. w_{Ra}, w_{Rb}, and w_{Rc} as,

$$w_{LRa}=\frac{w_{Ra}+w_{Rb}+w_{Rc}}{3} \tag{19}$$

The PI controller is fed with the difference of the nominal voltage and terminal voltage to generate the weight of terminal voltage error such that,

$$w_{Rt}(n+1)=w_{Rt}(n)+K_{p2}\{e_t(n+1)-e_t(n)\}+K_{i2}e_t(n+1) \tag{20}$$

$$\text{where } e_t(n)=V_t^*(n)-V_t(n) \tag{21}$$

The total reactive quadrature phase component is given as,

$$w_{Rs}=w_{Rt}-w_{LRa} \tag{22}$$

This weight is then used to generate the reactive component of

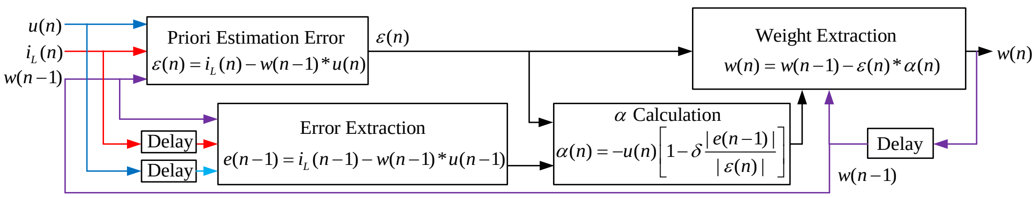

Fig. 2 Calculation of w(n).

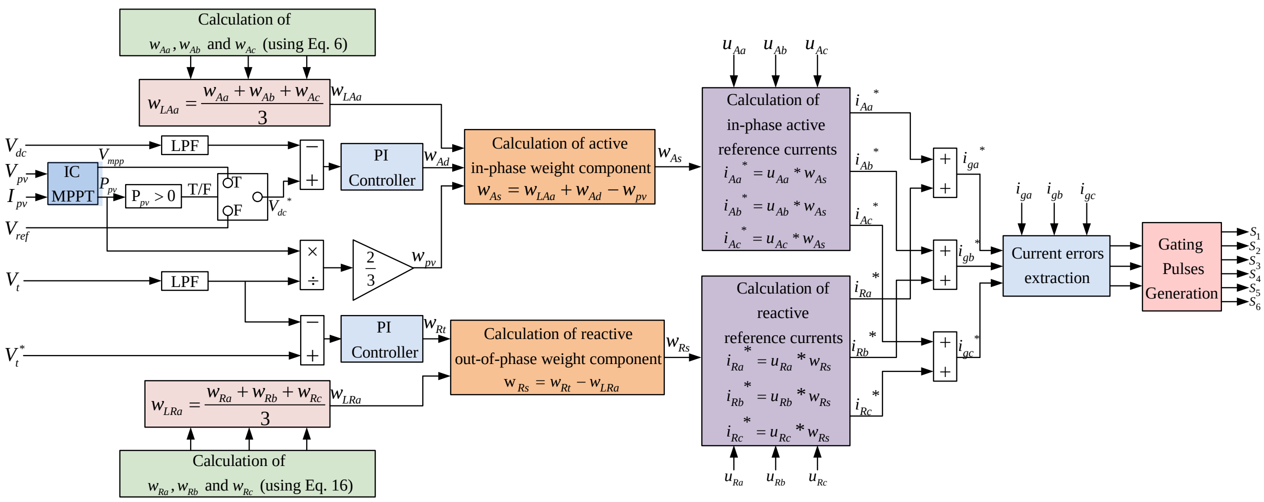

Fig. 3 Structure of control scheme.

This article has been accepted for publication in a future issue of this journal, but has not been fully edited. Content may change prior to final publication. Citation information: DOI 10.1109/TIA.2018.2867324, IEEE Transactions on Industry Applications

reference grid currents as,

$$i_{Ra}^* = u_{Ra} * w_{As}; i_{Rb}^* = u_{Rb} * w_{As}; i_{Rc}^* = u_{Rc} * w_{As} \quad (23)$$

The reference grid currents are then calculated as,

$$i_{ga}^* = i_{Aa}^* + i_{Ra}^*; i_{gb}^* = i_{Ab}^* + i_{Rb}^*; i_{gc}^* = i_{Ac}^* + i_{Rc}^* \quad (24)$$

These obtained reference currents and sensed grid currents are then compared in a hysteresis current controller for the generation of the VSC switching pulses.

IV. Simulation Results

The proposed second order Volterra filter based control is first validated in MATLAB/Simulink. A solar PV-DSTATCOM system consisting of solar PV array, three- phase grid, VSC and a nonlinear load, is modeled and is analyzed in power factor correction (PFC) mode. All parameters used for simulation are provided in Appendix.

A. System's Performance at Steady State with Nonlinear Load

Fig. 4 (a) depicts the waveform of I_{pv}, V_{pv}, P_{pv}, V_{dc}, P_g and Q_g while Fig. 4 (b) depicts the variation of v_g, i_g, i_{La}, i_{ga}^*, v_{spv} and i_{spv} at steady-state condition under a nonlinear load. The grid currents (i_g) are sinusoidal, although the load current is nonlinear (i_{La}). It is because of the compensation provided by VSC. As it can be seen, the solar PV extracts maximum power, and the system works in PFC mode. Fig. 4 (c) shows the THD in i_{La}, which is 25.74%. While Fig. 4 (d) shows the THD in i_{ga}, which is 1.69 %, below a limit of the IEEE-519 standard [7].

B. System's Dynamic Behavior at Unbalanced Nonlinear Load

Fig. 5 (a) shows the impact on V_{dc}, v_{gabc}, i_g, i_L, i_g^*, v_{spv} and i_{spv}, as the load in phase 'a' is disconnected. At t= 0.52 s, as the load is disconnected, i_{La} becomes zero. The VSC currents compensate the effect of load unbalance, maintaining sinusoidal grid currents in all three phases. Fig. 5 (b) depicts the variation of internal signals like ε_{Aa}, e_{Aa}, α_{Aa}, w_{LAa}, w_{pv}, w_{Ad} and w_{As} as the load is disconnected in phase 'a'. w_{LAa} and w_{As} are decreased as the load is disconnected.

C. System's Dynamic Behavior at Variable Solar Insolation

Fig. 6 (a) illustrates an impact of changing the solar insolation on G_{pv}, I_{pv}, V_{pv}, P_{pv}, V_{dc} and P_g. A decrease in G_{pv} from 1000 W/m^2 to 800 W/m^2 leads to a decrease in I_{pv} and thus in P_{pv}. Fig. 6 (b) shows a change in v_g, i_g, i_{La}, i_g^*, v_{spv} and i_{spv}. The decrease in grid currents (i_g) is compensated by an increase in VSC currents (i_{spv}), while load currents remain same (i_L).

D. Comparison of Proposed Control Technique with Conventional Control Technique

Fig. 7 shows a comparison of proposed technique with synchronous reference frame theory (SRFT) and least mean square (LMS). As it is seen from the figure, when the load in phase 'a' is removed, the proposed technique has lower ripples than SRFT. Lower ripples verify the stability claim of proposed technique as herein, the error asymptotically converges to zero (Lyapunov stability theory). Moreover, both SRFT and proposed Volterra-filter based technique, have shorter settling times in comparison to LMS. Although the settling time for proposed technique is almost one cycle more than SRFT, but a reduction in ripples is much more dominant.

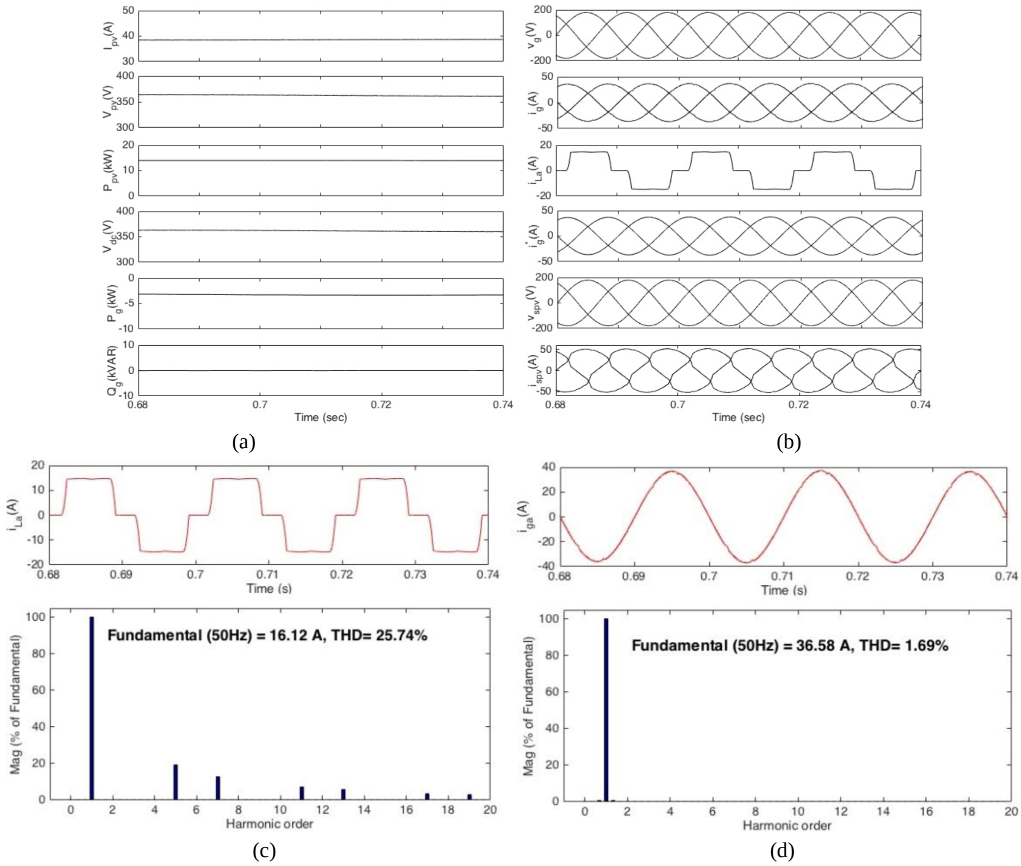

Fig. 4 (a-b) Steady state behavior with nonlinear load, (c) Harmonic analysis of load current, (d) Harmonic analysis of grid current.

This article has been accepted for publication in a future issue of this journal, but has not been fully edited. Content may change prior to final publication. Citation information: DOI 10.1109/TIA.2018.2867324, IEEE Transactions on Industry Applications

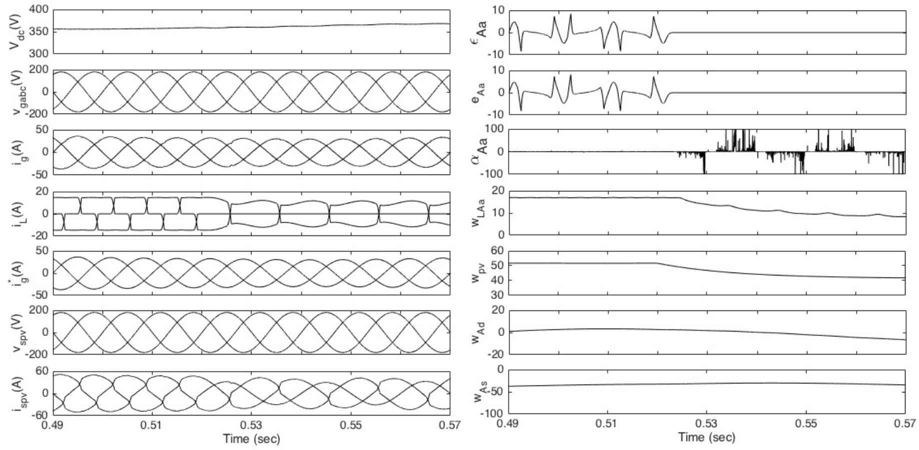

(a) (b)

Fig. 5 (a) Dynamic behavior under load removal and (b) Response of internal signals.

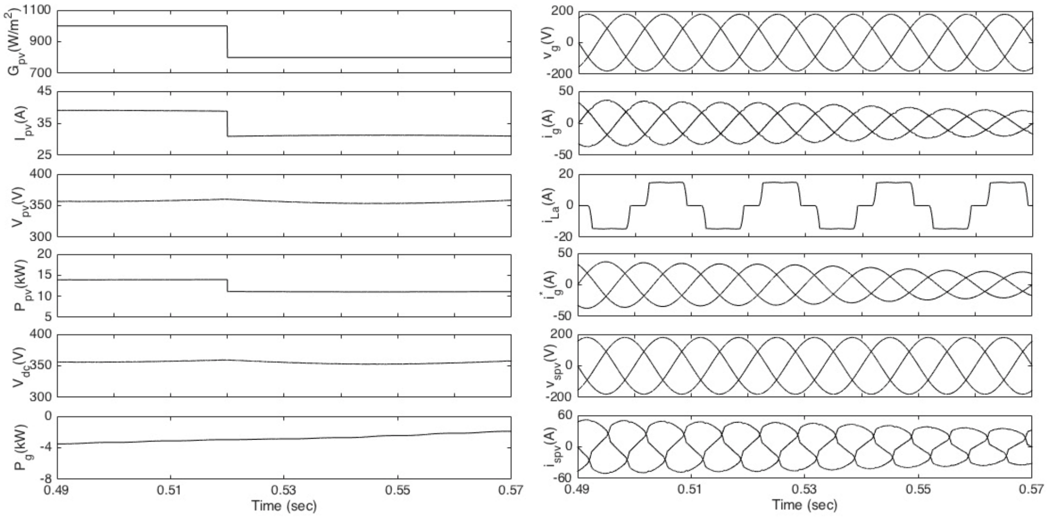

(a) (b)

Fig. 6 Dynamic behavior with decrease in solar insolation.

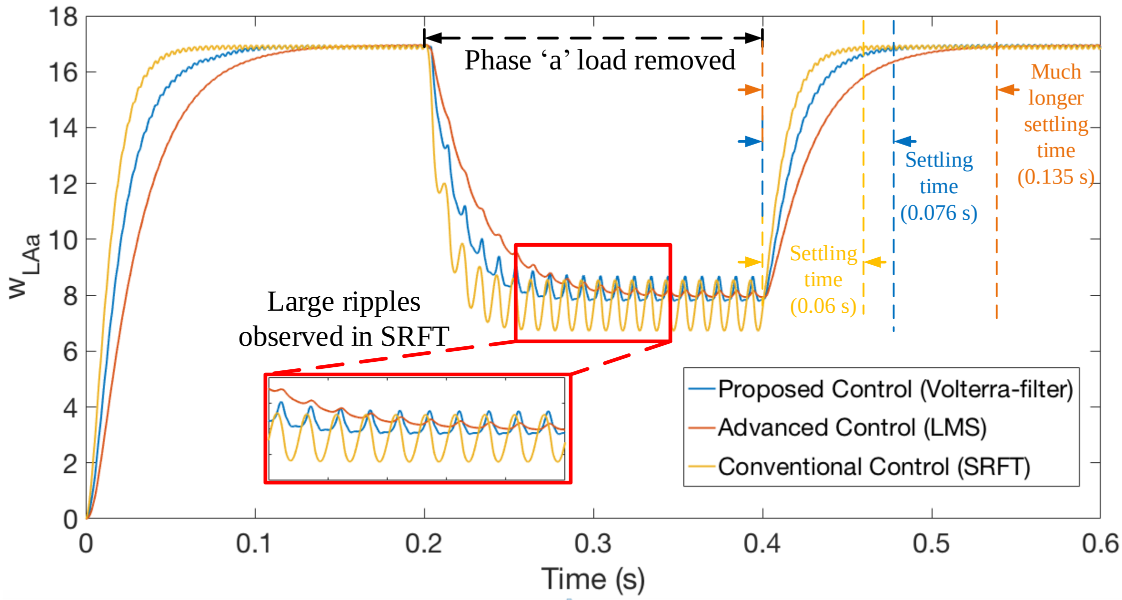

Fig. 7 Comparison of the proposed technique with synchronous reference frame theory (SRFT) and least mean square (LMS).

V. Experimental Results

A prototype of proposed PV-DSTATCOM system is developed. The system is realized using a solar PV simulator (AMETEK made ETS600x17DPVF). Hall-Effect based current sensors (LA 55- P) and voltage sensors (LV 25-P) are used to sense currents and voltages, respectively. A power analyzer (Fluke made 43B) is used along with four–channel

This article has been accepted for publication in a future issue of this journal, but has not been fully edited. Content may change prior to final publication. Citation information: DOI 10.1109/TIA.2018.2867324, IEEE Transactions on Industry Applications

DSO (Agilent made DSO7014A) to record the waveforms. The proposed control scheme is executed using DSP-dSPACE-1202 MicroLabBox. Parameters of the system, are stated in Appendix.

A. System's Behaviour under Steady State

The performance of solar PV-DSTATCOM system at steady state condition is shown in Figs. 8-9. Figs. 8(a-b) depict the grid voltage (v_{gbc}) and grid phase current (i_{ga}), harmonic spectrum and THD (Total Harmonic Distortion) of i_{ga}. The THD of i_{ga} is 3.1% which meets the IEEE-519 standard [7]. Figs. 8(c-d) depict v_{gbc} and load current of phase 'a' (i_{La}), THD of i_{La}, while Fig. 8(e) shows v_{gbc} and VSC phase current (i_{aspv}). Figs. 8(f-h) depict the power delivered by the grid, power consumed by the load and VSC power. Fig. 9 shows the waveforms of grid line voltage (v_{gbc}), phase 'c' grid current (i_{gc}), phase 'c' load current (i_{Lc}), and the VSC current in phase 'c' (i_{cspv}). As it is observed, the load current is non-sinusoidal but the grid current is maintained to be sinusoidal.

B. Behavior of the System as Phase 'a' Load is Disconnected

Figs. 10(a-d) depict the behavior of the system as the load is disconnected from phase 'a', making the system unbalanced. Fig. 10(a) shows the waveforms of DC link voltage (V_{dc}), i_{La}, i_{ga}, and i_{aspv}. Fig. 10(b) shows an impact of load disconnection on v_{gbc}, and parameters of phase 'c' like i_{gc}, i_{Lc} and i_{cspv}. Fig. 10(c) shows a variation of internal signals like e_{Aa}, ε_{Aa}, α_{Aa} and w_{Aa} with the change in loads. Fig. 10(d) shows the impact on the weights of the system as w_{Ad}, w_{pv}, w_{LAa} and w_{As}. The w_{LAa} component decreases to zero at disconnection of the load.

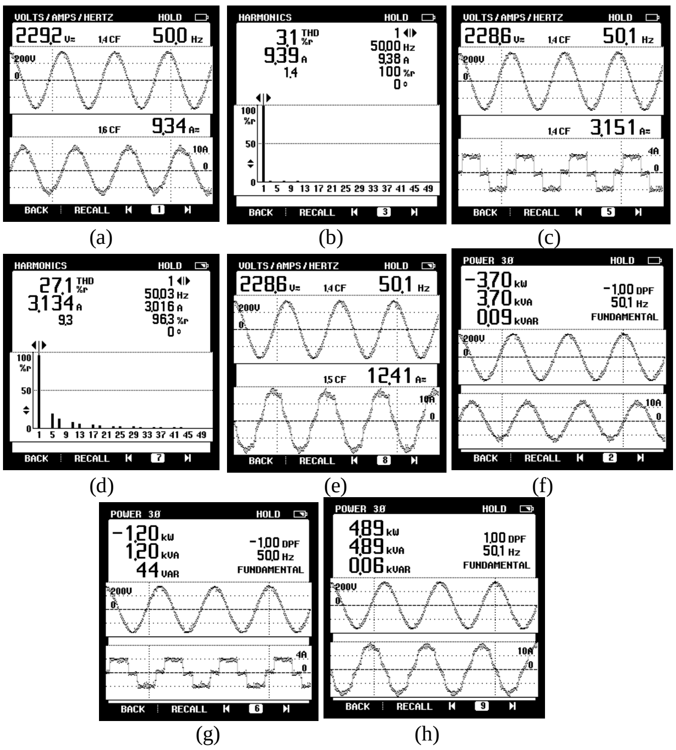

Fig. 8 (a) Grid voltage (v_{gbc}) and grid phase current (i_{ga}), (b) harmonic spectrum of i_{ga}, (c) v_{gbc} and load current of phase 'a' (i_{La}), (d) harmonic spectrum of i_{La}, (e) v_{gbc} and compensator phase current (i_{aspv}) (f-h) grid power, load power, compensator power.

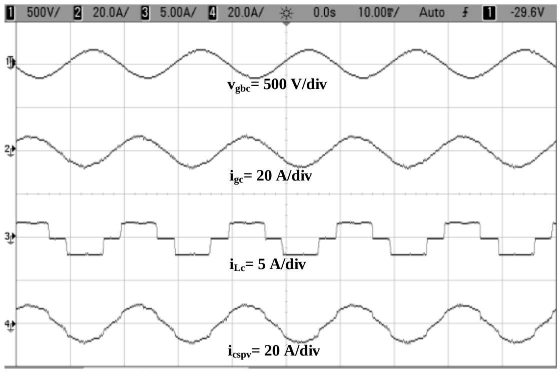

Fig. 9 Behavior of the system at steady state.

C. Impact of Increased Solar Insolation

Figs. 11(a-b) show the system's behavior as the solar insolation increases from 700 W/m^2 to 1000 W/m^2. Fig. 11(a) depicts the PV voltage (V_{pv}), PV current (I_{pv}), i_{aspv} and i_{ga}. The increase in insolation leads to an increase in I_{pv}. Fig. 11(b) depicts the impact on the weights of the system, w_{Ad}, w_{pv}, w_{LAa} and w_{As}. The w_{pv} component increases with the increase in PV insolation. Figs. 11(c-d) show 100% maximum power tracking at 700 W/m^2 and 1000 W/m^2, respectively.

VI. Lyapunov Stability Analysis

For system's stability analysis, the adaptation gain α(n) is changed as,

$$\alpha(n) = -\mathrm{u}(n)\left[1 - \frac{|e(n-1)|}{\lambda^{\frac{n}{2}}|\varepsilon(n)|}\right] \quad (25)$$

such that λ>1. For a system to be stable as per Lyapunov stability criterion, a positive definite Lyapunov function (V(n)) should have a negative definite ΔV(n) [24]. Defining a positive definite quadratic Lyapunov function for this system as,

$$V(n) = \lambda^n e^2(n) \quad (26)$$

Then,

$$\Delta V(n) = V(n) - V(n-1)$$

$$= \lambda^n \underline{e^2(n)} - \lambda^{n-1} e^2(n-1)$$

$$= \lambda^n \left[i_L(n) - \underline{w(n)}u(n)\right]^2 - \lambda^{n-1} e^2(n-1)$$

$$= \lambda^n \left[i_L(n) - \left\{w(n-1) - \varepsilon(n)\underline{\alpha(n)}\right\}u(n)\right]^2 - \lambda^{n-1} e^2(n-1)$$

$$= \lambda^n \left[i_L(n) - \left\{w(n-1) + \varepsilon(n)\mathrm{u}(n)\left(1 - \frac{|e(n-1)|}{\lambda^{\frac{n}{2}}|\varepsilon(n)|}\right)\right\}u(n)\right]^2$$

$$- \lambda^{n-1} e^2(n-1)$$

$$= \lambda^n \left[\underline{i_L(n) - w(n-1)u(n)} - \varepsilon(n)\,||\,\mathrm{u}^2(n)\,||\left(1 - \frac{|e(n-1)|}{\lambda^{\frac{n}{2}}|\varepsilon(n)|}\right)\right]^2$$

$$- \lambda^{n-1} e^2(n-1)$$

$$= \lambda^n \left[\varepsilon(n) - \varepsilon(n)\left(1 - \frac{|e(n-1)|}{\lambda^{\frac{n}{2}}|\varepsilon(n)|}\right)\right]^2 - \lambda^{n-1} e^2(n-1)$$

This article has been accepted for publication in a future issue of this journal, but has not been fully edited. Content may change prior to final publication. Citation information: DOI 10.1109/TIA.2018.2867324, IEEE Transactions on Industry Applications

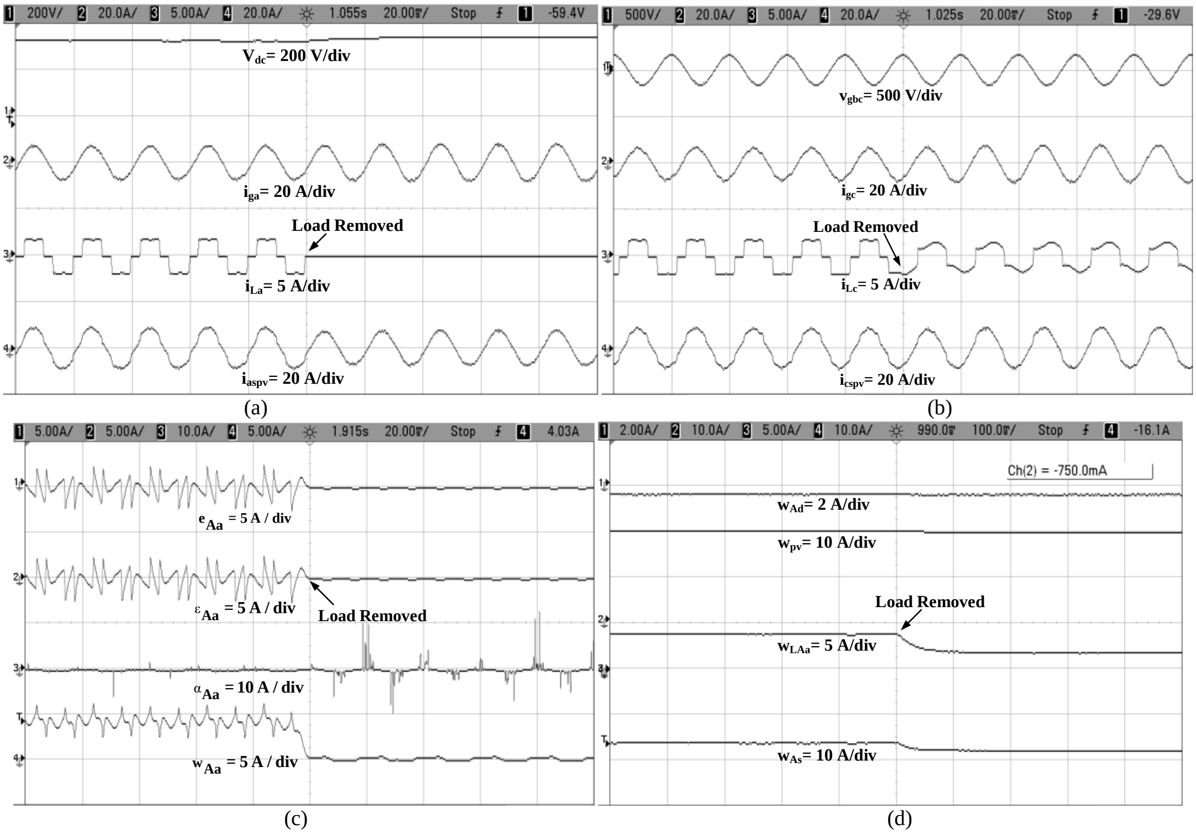

Fig. 10 Intermediate signals of control algorithm under load disconnection in the system.

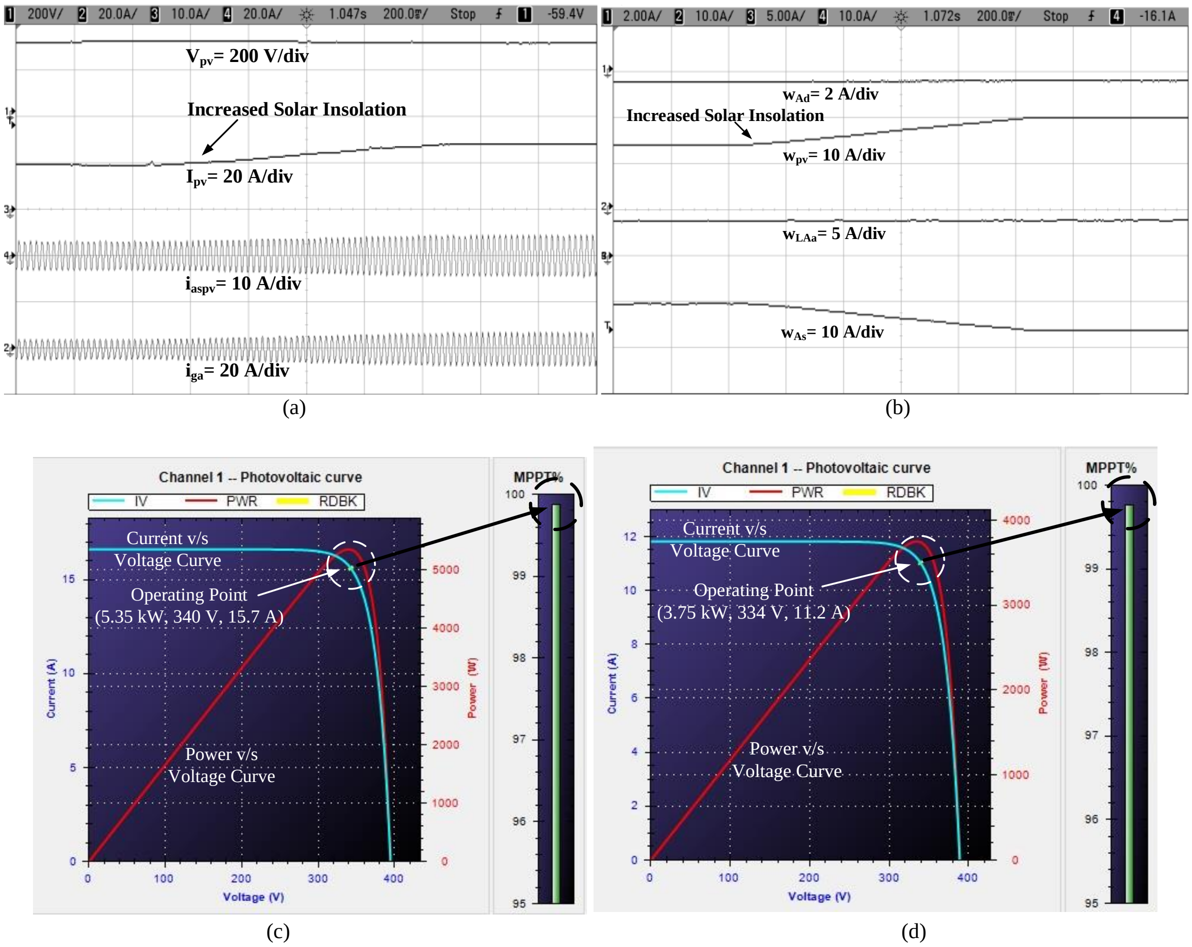

Fig. 11 (a-b) Impact of rise of solar insolation level, (c) tracking of maximum power by solar PV array at 1000 W/m^2, (d) tracking of maximum power by solar PV array at 700 W/m^2.

$$= \lambda^{n}\left[\varepsilon(n)\left(1-1+\frac{|e(n-1)|}{\lambda^{\frac{n}{2}}\,|\varepsilon(n)|}\right)\right]^{2}-\lambda^{n-1}e^{2}(n-1)$$

$$= \lambda^{n}\left[\varepsilon^{2}(n)\frac{|e^{2}(n-1)|}{\lambda^{n}\,|\varepsilon(n)|^{2}}\right]-\lambda^{n-1}e^{2}(n-1)$$

$$= e^{2}(n-1)-\lambda^{n-1}e^{2}(n-1)$$

$$= \left(1-\lambda^{n-1}\right)e^{2}(n-1) \qquad (27)$$

For n>1 and λ>1, ΔV(n) is negative definite, therefore, the error asymptotically converges to zero from Lyapunov stability theory.

VII. Conclusion

The solar PV-DSTATCOM system integrated to the distribution system, has been studied using second-order Volterra filter based control under various conditions like load disconnection and variable PV insolation. The solar PV array has been operated at maximum power using an IC-MPPT algorithm. The second-order Volterra filter based control is shown to be stable as per the Lyapunov's stable criterion. The developed control is easy to be implemented. Moreover, the error of the system also converges exponentially to zero asymptotically and thus helps in obtaining fast response. The observed THD value of grid currents are found well under the limit of the IEEE-519 standard. Moreover, the solar PV-DSTATCOM system shows DSTATCOM capabilities even in the absence of solar PV generation.

Appendix

Simulation Parameters: Solar PV array voltage= 360 V; array power= 11 kW; DC bus voltage, V_{dc}= 360 V; ripple filter R_f= 5 Ω, C_f= 10 μF,; L_f= 2.5 mH; C_{dc}= 12 mF; grid voltage, V_{LL}= 220 V (rms); PI controller, K_{p1}= 0.6, K_{i1}= 5, K_{p2}= 1, K_{i2}= 0, δ=0.65, non-linear load= 3-phase diode bridge, R= 20Ω, L= 100mH load.

Hardware Parameters: Sampling time, T_s= 35 μs; grid voltage, V_{LL}= 240 V (rms); V_{dc}= 340 V; VSC= 25 kVA; solar PV simulator voltage, V_{MPP}= 340 V; array current, I_{MPP}= 15.7 A; N_s = 12; N_p = 2 ; array power, P_{MPP}= 5.35 kW; DC bus voltage, ripple filter R_f= 5 Ω, C_f= 10 μF; interfacing inductor, L_f= 2.9 mH; PI controller, K_{p1}= 0.12, δ=0.9, non-linear load= diode bridge with 1.20 kW load.

Acknowledgments

The authors thank the DST, Govt. of India, for their support for this project under Grant Number: RP02979.

References

[1] H. Kirkham, D. Nightingale and T. Koerner, "Energy Management System Design with Dispersed Storage and Generation," *IEEE Transactions on Power Apparatus and Systems*, vol. PAS-100, no. 7, pp. 3432-3441, 1981.

[2] Richard D. Tabors, Susan Finger and Alan J. Cox, "Economic operation of distributed power systems within an electric utility," *IEEE Trans. Power Apparatus and Systems*, vol. PAS-100, no. 9, pp. 4186-4195, 1981.

[3] Benjamin Kroposki and Barry Mather, "Rise of distributed power: integrating solar energy into the grid," *IEEE Power and Energy Magazine*, vol. 13, no. 2, pp. 14-18, 2015.

[4] M. Karimi, H. Mokhlis, K. Naidu, S. Uddin and A.H.A. Bakar, "Photovoltaic penetration issues and impacts in distribution network—A review," *Ren. Sustainable Energy Review*, vol. 53, pp. 594–605, Jan. 2016.

[5] Xiaodong Liang, "Emerging power quality challenges due to integration of renewable energy sources," *IEEE Transactions on Industry Applications*, vol. 53, no. 2, pp. 855-866, 2017.

[6] Yuan-Kang Wu, Guan-Ting Ye and Mohamed Shaaban, "Analysis of impact of integration of large PV generation capacity and optimization of PV capacity: Case studies in Taiwan, " *IEEE Transactions on Industry Applications*, vol. 52, no. 6, pp. 4535 – 4548, 2016.

[7] IEEE Recommended practices and requirement for harmonic control on electric power system, IEEE Standard 519, 1992.

[8] IEEE Standard for Interconnecting Distributed Resources With Electric Power Systems, IEEE Std.1547, 2003.

[9] Moacyr Aureliano Gomes de Brito, Luigi Galotto, Leonardo Poltronieri Sampaio; Guilherme de Azevedo e Melo and Carlos Alberto Canesin, "Evaluation of the main MPPT techniques for photovoltaic applications," *IEEE Trans. Industrial Elect.*, vol. 60, no. 3, pp. 1156-1167, March 2013.

[10] T. Esram and P. L. Chapman, "Comparison of Photovoltaic Array Maximum Power Point Tracking Techniques," *IEEE Transactions on Energy Conversion*, vol. 22, no. 2, pp. 439-449, June 2007.

[11] G. J. Kish, J. J. Lee and P. W. Lehn, "Modelling and control of photovoltaic panels utilising the incremental conductance method for maximum power point tracking," *IET Renewable Power Generation*, vol. 6, no. 4, pp. 259-266, July 2012.

[12] Arindam Ghosh and Gerard Ledwich, "Load compensating DSTATCOM in weak AC systems," *IEEE Trans. on Power Delivery*, vol. 18, no. 4, pp. 1302-1309, Oct. 2003.

[13] B. Singh, A. Chandra and K. Al-Haddad, *Power quality: problems and mitigation techniques*, John Wiley & Sons Ltd., U.K, 2015.

[14] Bhim Singh, P. Jayaprakash, D. P. Kothari, Ambrish Chandra, and Kamal Al Haddad, "Comprehensive study of DSTATCOM configurations," *IEEE Trans. on Industrial Informatics*, vol. 10, no. 2, pp. 854 – 870, May 2014.

[15] Rajendra R. Sawant and Mukul C. Chandorkar, "A multifunctional four-leg grid-connected compensator," *IEEE Transactions on Industry Applications*, vol. 45, no. 1, pp. 249-259, 2009.

[16] Sabha Raj Arya, Bhim Singh, Ram Niwas, Ambrish Chandra and Kamal Al-Haddad, "Power quality enhancement using DSTATCOM in distributed power generation system," *IEEE Transactions on Industry Applications*, vol. 52, no. 6, pp. 5203-5212, 2016.

[17] Hareesh Kumar Yada and M.S.R Murthy, "An improved control algorithm for DSTATCOM based on single-phase SOGI-PLL under varying load conditions and adverse grid conditions," in *Proc. of IEEE Inter. Conf. on Power Electronics, Drives & Energy Systems (PEDES)*, 2016.

[18] Mrutyunjaya Mangaraj and Anup Kumar Panda, "NBP-based icosϕ control strategy for DSTATCOM," *IET Power Electronics*, vol. 10, no. 12, pp. 1617 – 1625, 2017.

[19] Aser Asselin Loubassou, Youbing Zhang, Qijun and Yesen, "Enhancement of isolated distributed generation system power quality using DSTATCOM," in *Proc. of 36th Chinese Control Conference (CCC)*, pp. 9278 – 9284, 2017.

[20] Li Tan and Jean Jiang, "Adaptive volterra filters for active control of nonlinear noise processes," *IEEE Trans. on Signal Processing*, vol. 49, no. 8, pp. 1667-1676, Aug. 2001.

[21] N. Beniwal, I. Hussain and B. singh, "A second-order volterra filter based control of SPV-DSTATCOM system to achieve Lyapunov's stability," in *Proc. of IEEE 7th Power India Inter. Conf. (PIICON)*, pp. 1-5, 2016.

[22] Z. H. Man, H. R. Wu, S. Liu, and X. H. Yu, "A new adaptive backpropagation algorithm based on Lyapunov stability theory for neural networks", *IEEE Trans. Neural Networks*, vol. 17, no. 6, pp. 1580-1591, November, 2006.

[23] Haiquan Zhao, Jiashu Zhang, "Filtered-X lyapunov algorithm for nonlinear active noise control using second-order volterra filter," in *Proc. 11th IEEE International Conf. on Communication Technology*, pp. 497 - 500, 2008.

[24] C. T. Chen, *Linear system theory and design*, 3rd Edition, Oxford University Press, 1999.

[25] K. Y. Nikravesh and Richard G. Hoft, "Lyapunov stability analysis of thyristor inverter system," *IEEE Transactions on Industry Applications*, vol. IA-11, no. 2, pp. 158 – 164, 1975.

[26] Rahul Agarwal, Ikhlaq Hussain and B. Singh, "LMF based control algorithm for single stage three-phase grid integrated solar PV system," *IEEE Trans. Sustainable Energy*, vol. 7, no. 4, pp. 1379-1387, Oct. 2016.

Neha Beniwal (S'17) has received her B. Tech. degree in electrical engineering from National Institute of Technology, Kurukshetra, India in 2014 and her M. Tech. degree in power electronics, electrical machines & drives (PEEMD) from Indian Institute of Technology, Delhi in 2017. She is currently working toward the Ph.D. degree at the Interdisciplinary Graduate School, Nanyang Technological University, Singapore. Her research interests include power electronics, renewable energy, microgrid, power quality, electrical machines and drives.

Ms. Beniwal is a recipient of POSOCO Power System Awards (PPSA) awarded by Power System Operation Corporation Ltd. (POSOCO) in association with Foundation for Innovation and Technology Transfer (FIIT), Indian Institute of Technology, Delhi in 2018. She is also the recipient of Prof. A.K. Sinha Cash Prize and IEEE-PEDES'96 Award at the Annual Convocation of Indian Institute of Technology, Delhi in 2017.

Ikhlaq Hussain (M'14) was born in Doda, Jammu and Kashmir, India, in 1986. He received his B. E. (Electrical) from University of Jammu, Jammu, India, in 2009 and M. Tech. (Gold Medalist) in Electrical Power System Management from the Jamia Millia Islamia (A Central University), New Delhi, India, in 2012. He has submitted his Ph.D. thesis in the Department of Electrical Engineering, Indian Institute of Technology Delhi, New Delhi, India. From September 2012 to December 2012, he was a Lecturer with the Department of Electrical Engineering, National Institute of Technology Srinagar, India. On 19 th April 2017, he joined as Assistant Professor in the Department of Electrical Engineering, Institute of Technology, University of Kashmir, Srinagar, India. His areas of research interests include power electronics, power quality, custom power devices, renewable energy systems, power system management and microgrid.

Mr. Hussain was a recipient of the POSOCO power system award (PPSA) from Power System Operation Corporation (POSOCO) Limited, India and Foundation for Innovation and Technology Transfer (FITT) at Indian Institute of Technology Delhi in 2017, Gandhian Young Innovations Award in 2018, Outstanding Faculty researcher in the field of energy for 2017-2018. He has selected as young scientist for 3rd BRICS young scientist conclave from 25th – 29th June 2018 at Durban, South Africa by DST, Govt. of India. He was recipient of IEEE INDICON Best Paper Award in 2015 and the IEEE UPCON Best Paper Award in 2016. He has published more than 100 papers in reputed journals and conferences. He is a contributing reviewer of a number of IEEE/IET/Elsevier journals and conferences.

Bhim Singh (SM'99, F'10) was born in Rahamapur, Bijnor (UP), India, in 1956. He has received his B.E. (Electrical) from the University of Roorkee, India, in 1977 and his M.Tech. (Power Apparatus & Systems) and Ph.D. from the Indian Institute of Technology Delhi, India, in 1979 and 1983, respectively.

In 1983, he joined the Department of Electrical Engineering, University of Roorkee (Now IIT Roorkee), as a Lecturer. He became a Reader there in 1988. In December 1990, he joined the Department of Electrical Engineering, IIT Delhi, India, as an Assistant Professor, where he has become an Associate Professor in 1994 and a Professor in 1997. He has been ABB Chair Professor from September 2007 to September 2012. He has also been CEA Chair Professor from October 2012 to September 2017. He has been Head of the Department of Electrical Engineering at IIT Delhi from July 2014 to August 2016. Since, August 2016, he is the Dean, Academics at IIT Delhi. He is JC Bose Fellow of DST, Government of India since December 2015.

Prof. Singh has guided 69 Ph.D. dissertations, and 167 M.E./M.Tech./M.S.(R) theses. He has been filed 29 patents. He has executed more than eighty sponsored and consultancy projects. He has co-authored a text book on power quality: *Power Quality Problems and Mitigation Techniques* published by John Wiley & Sons Ltd. 2015.

His areas of interest include solar PV grid interface systems, microgrids, power quality monitoring and mitigation, solar PV water pumping systems, improved power quality AC-DC converters, power electronics, electrical machines, drives, FACTS, and high voltage direct current (HVDC) systems.

Prof. Singh is a Fellow of the Indian National Academy of Engineering (FNAE), The Indian National Science Academy (FNA), The National Academy of Science, India (FNASc), The Indian Academy of Sciences, India (FASc), The World Academy of Sciences (FTWAS), Institute of Electrical and Electronics Engineers (FIEEE), the Institute of Engineering and Technology (FIET), Institution of Engineers (India) (FIE), and Institution of Electronics and Telecommunication Engineers (FIETE) and a Life Member of the Indian Society for Technical Education (ISTE), System Society of India (SSI), and National Institution of Quality and Reliability (NIQR).

He has received Khosla Research Prize of University of Roorkee in the year 1991. He is recipient of JC Bose and Bimal K Bose awards of The Institution of Electronics and Telecommunication Engineers (IETE) for his contribution in the field of Power Electronics. He is also a recipient of Maharashtra State National Award of Indian Society for Technical Education (ISTE) in recognition of his outstanding research work in the area of Power Quality. He has received PES Delhi Chapter Outstanding Engineer Award for the year 2006. Professor Singh has received Khosla National Research Award of IIT Roorkee in the year 2013. He is a recipient of Shri Om Prakash Bhasin Award-2014 in the field of Engineering including Energy & Aerospace. Professor Singh has also received IEEE PES Nari Hingorani Custom Power Award-2017.

He has been the General Chair of the 2006 IEEE International Conference on Power Electronics, Drives and Energy Systems (PEDES'2006), General Co-Chair of the 2010 IEEE International Conference on Power Electronics, Drives and Energy Systems (PEDES'2010), General Co-Chair of the 2015 IEEE International Conference (INDICON'2015), General Co-Chair of 2016 IEEE International Conference (ICPS'2016) held in New Delhi.